CoreDeep: Improving Crack Detection Algorithms Using Width Stochasticity

Ram Krishna Pandey, *Member, IEEE,* and Akshit Achara

Abstract—Automatically detecting or segmenting cracks in images can help in reducing the cost of maintenance or operations. Detecting, measuring and quantifying cracks for distress analysis in challenging background scenarios is a difficult task as there is no clear boundary that separates cracks from the background. Developed algorithms should handle the inherent challenges associated with data. Some of the perceptually noted challenges are color, intensity, depth, blur, motion-blur, orientation, different region of interest (ROI) for the defect, scale, illumination, complex and challenging background, etc. These variations occur across (crack inter class) and within images (crack intra-class variabilities). Overall, there is significant background (inter) and foreground (intra-class) variability. In this work, we have attempted to reduce the effect of these variations in challenging background scenarios. We have proposed a stochastic width (SW) approach to reduce the effect of these variations. Our proposed approach improves detectability and significantly reduces false positives and negatives. We have measured the performance of our algorithm objectively in terms of mean IoU, false positives and negatives and subjectively in terms of perceptual quality.

Keywords—Crack detection, Unet, segmentation, focal loss.

I. INTRODUCTION AND RELATED WORKS

AUTOMATIC crack detection is an important task in detecting, localizing and fixing the cracks. Structures that are subjected to cyclic load, fatigue stress results in cracks. Early detection of cracks allows us to take preventive measures for possible failures [1]. Cracks are a common defect category in many distress analysis tasks ranging from road inspection to estimating the remaining useful life of the material, object, surface or parts. In most of the cases, experts are needed to localize, measure and quantity cracks to fix it. Manual process is very tedious, challenging and error prone. Numerous computer vision method have been applied to detect cracks in an image. These algorithms can be broadly categorized into thresholding based [2], handcrafted feature based such as local binary pattern [3], histogram of oriented gradients [4], wavelets [5], gabor filters [6]. These features capture the local information but misses the global context. Crack detection using global view [7] takes in account geometric and photo-metric characteristics help in better connectivity. However, the performance drops significantly in challenging background situations.

Recently, deep learning techniques have shown promising results in various computer vision tasks such as semantic segmentation, object detection and classification. These algorithms extract features in hierarchical form from low level representation to high level. These features are extracted from data to capture local as well as global feature representation

Ram Krishna Pandey and Akshit Achara are with GE Research, Bangalore, India

of an image that helps in solving many challenging problems. In [8], the authors have shown that the performance of algorithms can be improved at three different levels i.e. input, architecture, and the objective followed by post-processing. In [9], the authors have shown randomly dropping character pixels in input image can help better connecting strokes thereby improving OCR performance. In this work, we have explored input with better augmentation strategy [10], used two different backbone [11], [12] replacing the encoder of U-Net [13] using [14] as shown in Fig. 2 (architecture exploration). We have used binary cross entropy and focal loss [15] (objective exploration), to improve the performance of our crack detection algorithm by a significant margin.

A. Contributions

Following are our key contributions :

1. We advocate the use of stochastic dilation (see Fig. 1) to improve the crack detactability and connectivity (see results shown in Fig. 5 and 6).

2. We use focal loss [15] and random augmentation [10] to improve the performance over baseline by a significant margin.

3. We have used the idea of binning to obtain the threshold (see subsection III-A) optimize our crack prediction that further refines the predictions and improves the mean IoU [16].

4. We have used different backbones [11], [12] to show the effectiveness of our approach on two different feature extractor. Tables I and III lists the results obtained using our approaches.

5. Our method significantly reduces false positive (FP) and false negative (FN) (refer section III-B for FP and FN computation) by a significant margin (see Tables I and III).

II. DATASETS USED FOR STUDY

We have used Kaggle crack segmentation dataset [17], [18], [19], [20], [21], [22], [23] that has around 11298 images. These images are obtained after merging 12 crack segmentation datasets. There are some 'noncrack' images present in the datasets. All the images are resized to a fixed size of (448, 448). Dataset is split into a train and test folders. The train folder contains 9603 images and test folder contains 1695 images. The splitting is stratified so that the proportion of each datasets in the train and test folder are similar.

A. Training and Validation

Figures 2 and 3 shows a detailed architecture diagram of the model used to obtain the results listed in Figures 5, 6 and Tables I, III, II and IV.
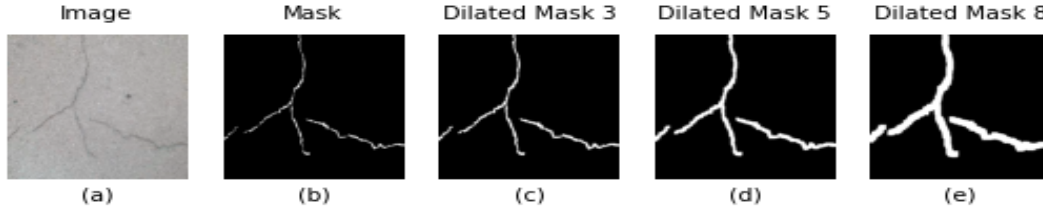
Fig. 1: Shows (a) original image, (b) ground truth, (c) dilated with mask 3×3, (d) dilated with mask 5×5 and (e) dilated with mask 8×8.

Fig. 2: Shows the model architecture (using resnet50 [11] backbone) diagram that is used to obtain the results.

Fig. 3: Shows the architecture (using efficientnetb4 [12] backbone) diagram that is used to obtain the results.

In all our experiments, we divided the train dataset into train and validation. We created the validation set from train folder aggregating 20 percent of the images from each of the 12 crack segmentation datasets. We have used a fixed validation set for all our experiments, so that we can show the performance improvement obtained is due to stochastic width approach we followed. The results reported in the tables I, III, II, and IV and Figures 5, 6 are obtained on the separate test data.

III. EXPERIMENTS

Fig. 1 shows an example image of the dilated mask images obtained for each crack image. We assume that (a) there is a fuzziness in the boundaries of crack and can be easily missed while marking the crack pixels (human error). (b) There is a variability in the width of the crack which is seen across different datasets (e.g. see fig. 5a and 5b taken from two different datasets. Fig. 5a is thinner compared to 5b) and within each image (e.g see in fig. 5a top right portion of the crack the image is thin and faint compared to other region of the crack). Incorporating width stochasticity allows the algorithm to learn the width variabilities across and within multiple datasets.

Figures 5b, 5c, 5d, 5e, 5f, 5g, 5h, 5i and 5j compares the results obtained using our methods and the ground truth masks. These results are obtained using resnet50 [11] as backbone. To show the improvement of our approach over the baseline and baseline+ (ref. section IV) we have fixed all other network parameter and trained the models: (a) baseline, (b) baseline+, our (c) stochastic width and (d) threshold operation performed on SW masks ; experiments in same working conditions (see captions of the Figures 5 and 6 for more details).

Similarly, Figures 6b, 6c, 6d, 6e, 6f, 6g, 6h, 6i and 6j compares the results obtained using our methods and the ground truth masks. These results are obtained using efficient-netb4 [12] as backbone architecture (see captions of the figures for more details).

We have performed experiments with custom UNet architecture shown in Figure 2 and 3. We have used resnet50 [11] and efficientnet [12] trained weights on imagenet [24] dataset as a backbone to initialise the network. We have used keras binary cross-entropy and segmentation model binary focal dice loss. Augmentation strategy is random augmentation [10] from the list of augmentations flip, rotate, brightness contrast, shiftScaleRotate, shear, scale, translate, multiplicativeNoise, randomGamma, downScale, HueSaturationValue, CLAHE, channel dropout, coarse dropout [25], color jitter, gaussian blur, median blur, grid dropout, maskDropout. The optimizer used is adam [26] with an initial learning rate of 1e-3. We used the ReduceLROnPlateau learning rate callback to adjust the learning rate based on the change in validation loss. After every 50 epochs, the learning rate was reduced by 0.5 with a minimum possible learning rate of 1e-6.

A. Threshold selection

We have used the numpy.argmax function for calculating the labels from prediction probabilities. We have also analyzed the

prediction probabilities from the model to obtain the predictions with high probabilities (strong candidate pixels for cracks) and the predictions with low probability (weak candidate pixels for cracks). We have performed an experiment on the validation dataset where we obtain the crack probabilities for all the pixels in an image. We then created 10 equally sized bins starting from min probability to maximum to understand the distribution of the probabilities. We start from minimum probability value and keep increasing the threshold (to next bin) till the number of connected components (cracks) is more than the initial prediction. This will happen if algorithms start disconnecting faint or thinner cracks, thereby increasing the total number of cracks in an image. We calculated the threshold for each image (except "noncrack" images) in the validation set and then obtain the distribution of these thresholds. We created 10 bins from these thresholds and found that the most common threshold values lie in the 10th bin, so we chose the mean value of 0.95 using the last bin boundaries (0.899 and 0.999). We then predicted on the images by using the thresholds (around the average threshold value calculated previously) 0.90 to 0.98 at an interval of 0.01. We observed that the weaker predictions were removed and the Crack IoU was significantly improved using this thresholding technique. This approach worked well on both the baseline models and resulted in an increased IoU in both the cases.

### B. Image Level False Positives and False Negatives

The approach to compute false positives and false negatives listed in the tables I and III are as follows; if the model predicts a crack even if there was no crack in the true mask and the image is FP. So, we count the number of 'noncrack' datasets images for which there was a crack predicted. The false negatives are computed by counting non crack predictions (misses) when there was actually a crack in the true mask and the image. FP and FN computation can be considered an alternative metric to access the performance of the algorithms in practical scenarios.

IV. RESULTS AND DISCUSSION

Table II list the quantitative results obtained by the models trained with and without stochastic width dilation and using resnet50 [11] as backbone. The model trained with stochastic dilation shows a significant improvement in terms of mean IoU at threshold=0.94. The FP has significantly reduced from 32 to 2 in SW experiment II.

Table I compares the results of baseline with our approaches. Column named 'Approach' list different approaches that we trained on crack segmentation datasets [17]. 'Baseline' is the model trained on crack segementation dataset [17] using binary cross entropy loss. Backbone used here is resnet50 [11]. Pre-trained weights is trained on image-net [24] datasets. Baseline+ is the model trained with focal loss [15] and random augmentation [10] from the list of augmentations (mention in section III) available in ablumenation library [27]. SW is model trained with focal loss, random augmentation and multiple dilation (as shown in Fig. 1). Multiple dilation here means the masks are dilated with 3, 5 and 8 using the dilate

Fig. 4: Shows the plot of threshold for each image in the validation set (crack images); (a) plot of thresholds for each crack image above 0.899 (model trained with efficientnetb4 backbone) (b) plot of thresholds for each crack images above 0.899 (model trained with resnet backbone), (c) plot of thresholds for all images (having cracks) and at all threshold (model trained with efficientnetb4 backbone) (b) plot of thresholds for all images (having cracks) and at all threshold (model trained with resnet50 backbone)
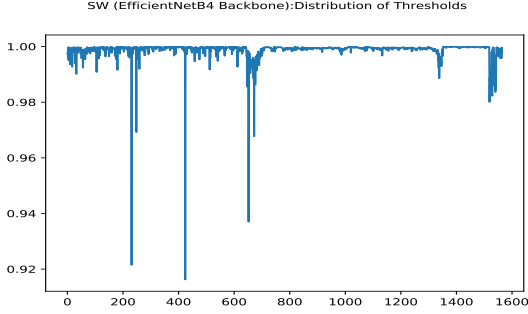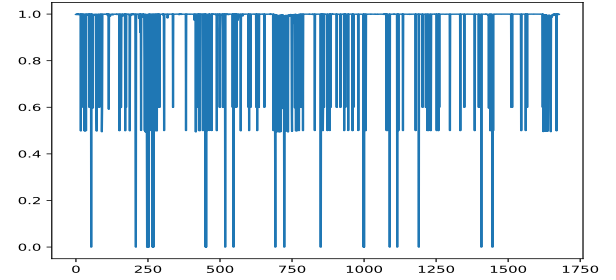

(a) Shows that the threshold distribution (from the bin: 0.899 to 0.999) of pixels in the prediction mask using the SW model trained using efficientnetb4 backbone
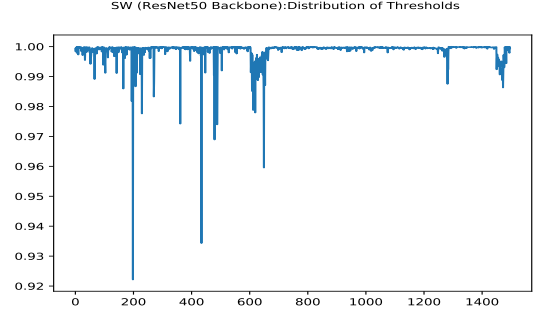
(b) Shows that the threshold distribution (from all bins: 0 to 0.999) of pixels in the prediction mask using the SW model trained using resnet50 backbone
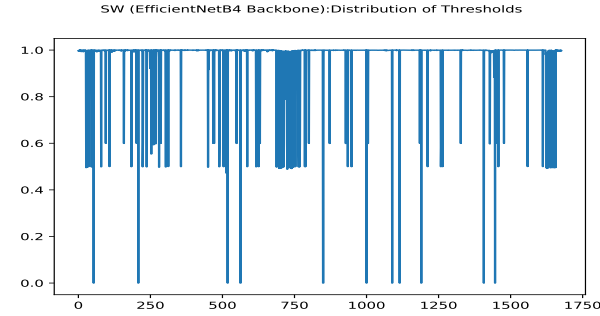
(c) Shows that the threshold distribution (from the bin: 0.899 to 0.999) of pixels in the prediction mask using the SW model trained using efficientnetb4 backbone

(d) Shows that the threshold distribution (from all bins: 0 to 0.999) of pixels in the prediction mask using the SW model trained using resnet50 backbone

TABLE I: Comparison of baseline with our proposed approaches. mIoU is mean IoU [16], mF1 is mean F1 score, FN is false negative, FP is false positive,C_IoU is crack IoU, C_P is crack precision, C_R is crack recall, C_F1 is crack F1 score and B_F1 is background F1 score
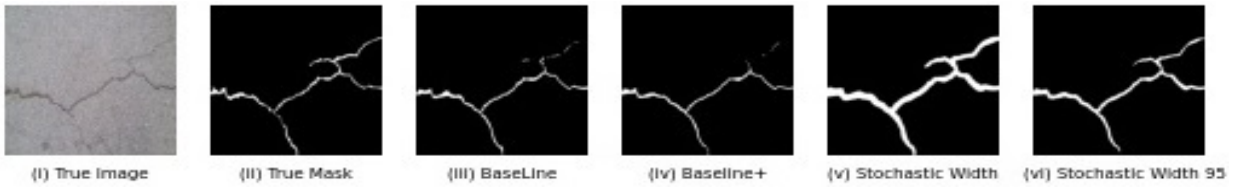
Approach	mIoU	mF1	FN	FP	C_IoU	B_IoU	C_P	C_R	C_F1	B_F1
Baseline	0.73	0.82	20	32	0.485	0.98	0.73	0.60	0.649	0.99
Baseline+	0.75	0.83	22	30	0.515	0.98	0.72	0.65	0.676	0.99
SW	0.71	0.80	16	11	0.464	0.96	0.51	0.89	0.624	0.98
SW_94	0.75	0.83	21	2	0.526	0.98	0.67	0.76	0.680	0.99
SW_95	0.75	0.83	22	2	0.526	0.98	0.68	0.74	0.680	0.99
SW_96	0.75	0.83	22	1	0.525	0.98	0.70	0.71	0.678	0.99

TABLE II: Comparison of our methods with baseline using backbone resnet50 [11] on multiple test datasets

Dataset	BaseLine	BaseLine+	SW	SW_94	**SW_95**	SW_96
GAPS384	0.282	0.331	0.366	0.333	0.315	0.29
CRACK500	0.552	0.584	0.578	0.555	0.547	0.534
forest	0.253	0.467	0.212	0.322	0.334	0.349
Sylvie	0.262	0.165	0.495	0.298	0.278	0.254
DeepCrack	0.669	0.684	0.491	0.625	0.634	0.645
Volker	0.585	0.601	0.548	0.66	0.664	0.666
cracktree200	0.109	0.04	0.059	0.113	0.121	0.131
Eugen	0.342	0.548	0.531	0.626	0.625	0.619
Rissbilder	0.474	0.503	0.395	0.525	0.533	0.54
CFD	0.276	0.459	0.186	0.287	0.299	0.315

function from the opencv-python library. This idea of dilating the mask of the crack with multiple dilation factor helps in capturing the width of the cracks with less misses and less false positives. Crack may have intra crack variabilities, such

(I) True Image (II) True Mask (III) BaseLine (Iv) Baseline+ (v) Stochastic Width (vi) Stochastic Width 95

(a) Shows example image from CFD [21] test dataset.

(b) Shows example image from crack 500 [18] test dataset.
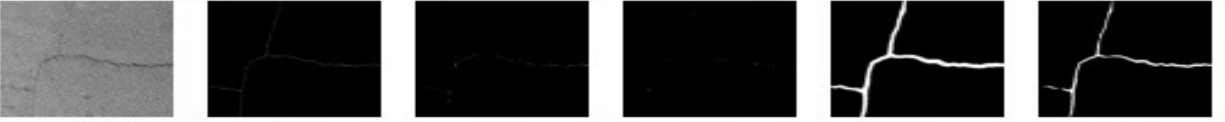
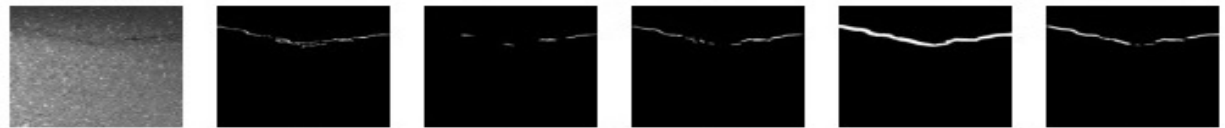(c) Shows example image from cracktree200 test dataset.

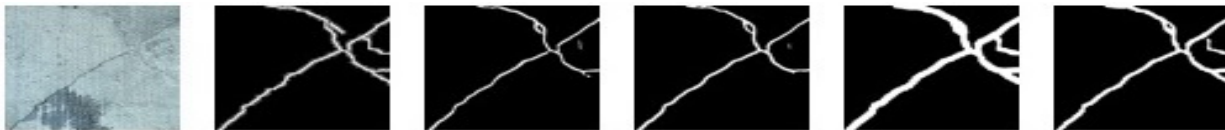(d) Shows example image from DeepCrack test dataset.

(e) Shows example image from Eugen Muller test dataset.

(f) Shows example image from forest test dataset

(g) Shows example image from GAPS384 test dataset

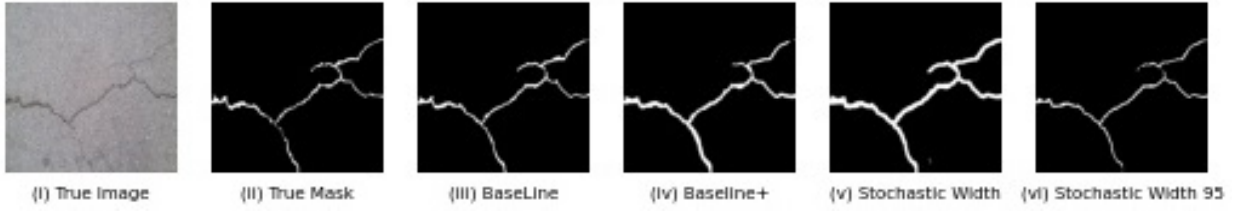(h) Shows example image from Rissbilder test dataset

(i) Shows example image from Sylvie Chambon test dataset

(j) Shows example image from Volker test dataset.

Fig. 5: Shows an example image from each dataset; from left to right : a) original image, (b) ground truth, (c) baseline, (d) baseline+ and (e) stochastic width (SW) (f) SW thresholded (at p=0.95) (trained using resnet50 backbone)

(I) True Image   (II) True Mask   (III) BaseLine   (Iv) Baseline+   (v) Stochastic Width   (vi) Stochastic Width 95

(a) Shows example image from CFD [21] test dataset.

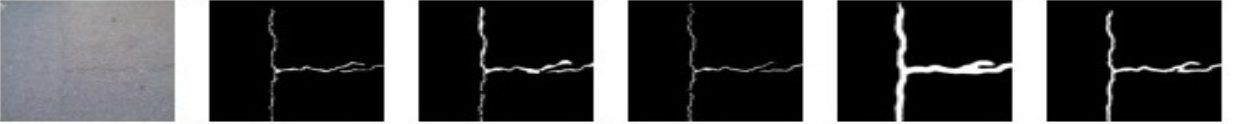(b) Shows example image from crack 500 [18] test dataset

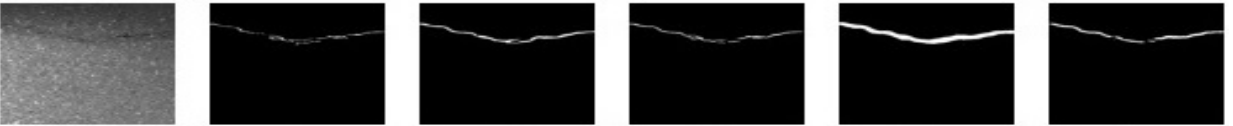(c) Shows example image from cracktree200 [7] test dataset.

(d) Shows example image from DeepCrack test dataset.

(e) Shows example image from Eugen Muller test dataset.

(f) Shows example image from forest test dataset

(g) Shows example image from GAPS384 [20] test dataset

(h) Shows example image from Rissbilder test dataset

(i) Shows example image from Sylvie Chambon test dataset
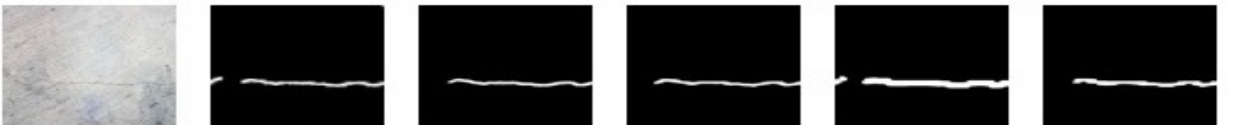
(j) Shows example image from Volker test dataset.

Fig. 6: Shows an example image from each dataset; from left to right : a) original image, (b) ground truth, (c) baseline, (d) baseline+ and (e) stochastic width (SW) (f) SW thresholded (at p=0.95) (trained using efficientnetb4 backbone)

TABLE III: Comparison of baseline (efficientnet) with our proposed approaches. mIoU is mean IoU, mF1 is mean F1, FN is false negative, FP is false positive,C_IoU is crack IoU, C_P is crack precision, C_R is crack recall, C_F1 is crack F1 score and B_F1 is background F1 score

Approach	mIoU	mF1	FN	FP	C_IoU	B_IoU	C_Precision	C_Recall	C_F1	B_F1
BaseLine	0.76	0.84	5	2	0.543	0.98	0.78	0.65	0.689	0.99
BaseLine+	0.77	0.85	15	6	0.557	0.98	0.73	0.71	0.705	0.99
SW	0.71	0.80	8	4	0.458	0.96	0.49	0.93	0.615	0.98
SW_94	0.76	0.84	11	2	0.550	0.98	0.66	0.81	0.699	0.99
SW_95	0.76	0.84	12	1	0.553	0.98	0.68	0.78	0.701	0.99
SW_96	0.77	0.84	11	1	0.552	0.98	0.70	0.75	0.700	0.99

TABLE IV: Comparison of our methods with baseline using backbone efficientnetb4 [12] on multiple test datasets

Dataset	BaseLine	BaseLine+	SW	SW_94	**SW_95**	SW_96
Sylvie	0.229	0.401	0.452	0.277	0.256	0.24
Eugen	0.602	0.612	0.496	0.618	0.625	0.631
CRACK500	0.591	0.625	0.574	0.609	0.604	0.596
cracktree200	0.076	0.028	0.079	0.176	0.179	0.169
Volker	0.65	0.66	0.527	0.656	0.663	0.67
DeepCrack	0.747	0.726	0.511	0.685	0.696	0.705
forest	0.432	0.317	0.231	0.381	0.398	0.415
Rissbilder	0.51	0.524	0.381	0.52	0.529	0.536
GAPS384	0.41	0.413	0.365	0.374	0.356	0.327
CFD	0.401	0.301	0.212	0.356	0.373	0.39

as some portion of the crack may be thick compared to the other portion that may have thinner or faint cracks. Capturing the width of the cracks helps the algorithms in predict full length of the cracks.

A. Observations

The images in Fig. 5 and Fig. 6 compares the predictions of the models; baseline, baseline+ and the ones obtained after training using our proposed idea of stochastic width and using thresholding to obtain better width prediction (III-A). In all the models we have shown the effectiveness of our proposed approach using two feature extractors/backbones resnet50 [11] and EfficientNetB4 [12]. We have observed for some images e.g. in the images that are taken from the datasets CRACK500 and cracktree200. Figures 5b, 6b, 5c and 6c shows that our predictions are better than that of the ground truth mask images. The image from Volker dataset 5j and 6j shows that the left side portion of the crack is captured better in stochastic width experiment compared to the other methods. Also, almost all the images in Figures 5 and 6 taken from multiple test datasets shows that our stochastic width approach captures the randomness in the cracks most effectively, thereby obtaining better connected cracks in comparison to the ones obtained from baseline and baseline+ methods where some portion of the cracks are getting missed.

Fig. 4 shows the threshold plot of all the images in the validation set (crack images). Fig. 4a shows the threshold plot of all the crack images in the validation dataset using the model trained with efficientnetb4 backbone (thresholds above 0.899). Similarly, Fig. 4b shows the threshold plot of all the crack images in the validation dataset using the model trained with resnet50 backbone (threshold above 0.899). Fig. 4c shows the threshold plot of all the crack images in the val dataset using the model trained with efficientnetb4 backbone (all calculated threshold values). Similarly, Fig. 4d shows the threshold plot of all the crack images in the val

dataset using the model trained with resnet50 backbone (all calculated threshold values). Plots show that most of the crack image thresholds are above 0.899 and efficientnetb4 model has around 1600 images while resnet50 model has around 1450 images above threshold 0.899. This implies that efficient net model is better compared to the resnet50 model. Plot also visually validates the idea of binning discussed in section III-A.

V. CONCLUSION

We have shown that judiciously combining traditional approaches in a deep learning framework can give significant boost in the performance of the crack detection algorithms. The proposed stochastic width approach results in better crack connectivity, reduces false positives and improves the crack detactability by a significant margin (see results Figures 5, 6 and tables I, III). We have further refined the predictions based on the probabilities of each pixel in predicted masks. The thresholded masks obtain better estimates of "crack width" which further refines the predictions, improves the perceptual quality (shown in Fig. 5 and 6), reduces the number of false positives (in terms of pixels), and improves the mean IoU [16] by a significant margin as listed in the tables I and IV.

REFERENCES

[1] Dhital, D., and Lee, J. R. A fully non-contact ultrasonic propagation imaging system for closed surface crack evaluation. Experimental mechanics, 52(8), 1111-1122 (2012).

[2] Liu, F., Xu, G., Yang, Y., Niu, X., Pan, Y. Novel approach to pavement cracking automatic detection based on segment extending. In International Symposium on Knowledge Acquisition and Modeling (pp. 610-614) (2008).

[3] Hu, Y., and Zhao, C. X. A novel LBP based methods for pavement crack detection. Journal of pattern Recognition research, 5(1), 140-147 (2010).

[4] Kapela, R., Śniatała, P., Turkot, A., Rybarczyk, A., Pożarycki, A., Rydzewski, P., Błoch, A. Asphalt surfaced pavement cracks detection based on histograms of oriented gradients. In IEEE 22nd International Conference Mixed Design of Integrated Circuits and Systems (MIXDES) (pp. 579-584) (2015).

[5] Zhou, J., Huang, P. S., and Chiang, F. P. Wavelet-based pavement distress detection and evaluation. Optical Engineering, 45(2), 027007 (2006).

[6] Xu, H., Su, X., Wang, Y., Cai, H., Cui, K., and Chen, X. (2019). Automatic bridge crack detection using a convolutional neural network. Applied Sciences, 9(14), 2867.

[7] Zou, Q., Cao, Y., Li, Q., Mao, Q., and Wang, S. CrackTree: Automatic crack detection from pavement images. Pattern Recognition Letters, 33(3), 227-238 (2012).

[8] Pandey, Ram Krishna, A. G. Ramakrishnan, and Souvik Karmakar. "Effects of modifying the input features and the loss function on improving emotion classification." TENCON 2019-2019 IEEE Region 10 Conference (TENCON). IEEE, 2019.

[9] Pandey, R. K., Vignesh, K., and Ramakrishnan, A. G, Chandrahasa B. Binary document image super resolution for improved readability and OCR performance. arXiv preprint arXiv:1812.02475 (2018).

[10] Cubuk, E. D., Zoph, B., Shlens, J., and Le, Q. V. Randaugment: Practical automated data augmentation with a reduced search space. In Proceedings of the IEEE/CVF conference on computer vision and pattern recognition workshops (pp. 702-703) (2020).

[11] He, K., Zhang, X., Ren, S., and Sun, J. (2016). Deep residual learning for image recognition. In Proceedings of the IEEE conference on computer vision and pattern recognition (pp. 770-778).

[12] Tan, M., and Le, Q. Efficientnet: Rethinking model scaling for convolutional neural networks. In International conference on machine learning (pp. 6105-6114). PMLR (2019).

[13] Ronneberger, O., Fischer, P., and Brox, T. U-net: Convolutional networks for biomedical image segmentation. In International Conference on Medical image computing and computer-assisted intervention (pp. 234-241). Springer, Cham (2015, October).

[14] https://github.com/yingkaisha/keras-unet-collection

[15] Lin, T. Y., Goyal, P., Girshick, R., He, K., and Dollár, P. Focal loss for dense object detection. In Proceedings of the IEEE international conference on computer vision (pp. 2980-2988) (2017).

[16] https://keras.io/api/metrics/segmentation_metrics/

[17] https://www.kaggle.com/datasets/lakshaymiddha/crack-segmentation-dataset

[18] Zhang, L., Yang, F., Zhang, Y. D., and Zhu, Y. J. Road crack detection using deep convolutional neural network. In 2016 IEEE international conference on image processing (ICIP) (pp. 3708-3712). IEEE.

[19] Yang, F., Zhang, L., Yu, S., Prokhorov, D., Mei, X., and Ling, H. Feature pyramid and hierarchical boosting network for pavement crack detection. IEEE Transactions on Intelligent Transportation Systems, 21(4), 1525-1535 (2019).

[20] Eisenbach, M., Stricker, R., Seichter, D., Amende, K., Debes, K., Sesselmann, M., ... and Gross, H. M. How to get pavement distress detection ready for deep learning? A systematic approach. In international joint conference on neural networks (IJCNN) (pp. 2039-2047), 2017.

[21] Shi, Y., Cui, L., Qi, Z., Meng, F., and Chen, Z. Automatic road crack detection using random structured forests. IEEE Transactions on Intelligent Transportation Systems, 17(12), 3434-3445, 2016.

[22] Amhaz, R., Chambon, S., Idier, J., and Baltazart, V. Automatic crack detection on two-dimensional pavement images: An algorithm based on minimal path selection. IEEE Trans. on Intelligent Transportation Systems, 17(10), 2718-2729, 2016.

[23] Zou, Q., Cao, Y., Li, Q., Mao, Q., and Wang, S. CrackTree: Automatic crack detection from pavement images. Pattern Recognition Letters, 33(3), 227-238, 2012.

[24] Deng, J., Dong, W., Socher, R., Li, L. J., Li, K., and Fei-Fei, L. Imagenet: A large-scale hierarchical image database. In 2009 IEEE conference on computer vision and pattern recognition (pp. 248-255). (2009).

[25] DeVries, T., and Taylor, G. W. (2017). Improved regularization of convolutional neural networks with cutout. arXiv preprint arXiv:1708.04552.

[26] Kingma, D. P., and Ba, J. Adam: A method for stochastic optimization. arXiv preprint arXiv:1412.6980.

[27] Buslaev, A., Iglovikov, V. I., Khvedchenya, E., Parinov, A., Druzhinin, M., and Kalinin, A. A. Albumentations: fast and flexible image augmentations. Information, 11(2), 125 (2020).